Bio-Medical Materials and Engineering 16 (2006) 67–75
IOS Press

Three-dimensional reconstruction and quantitative analysis of the brain stem nuclei based on fast centroid auto-registration

Yi-Chen Chen [a], Kuang-Hu Hu [a,*], Fang-Zhen Li [a], Wan-Fang Su [a] and Bao-Lin Zhang [b]
[a] *Institute of Biophysics, Chinese Academy of Sciences, Beijing 100101, China*
[b] *Laboratory of Neuropathology, Chengde Medical University, Chengde 067080, China*

Received 27 October 2004

Abstract. This paper introduces a three-dimensional (3D) reconstruction algorithm of the brain stem nuclei based on fast centroid auto-registration. The research is based on methods and theories of computer stereo vision, and by image information processing three-point pattern local search, registration and auto-tracing for the centroids of the brain stem nuclei were accomplished. We adopt two-peak threshold, edge detection and grayscale image enhancement to extract contours of the nuclei's structures. The experimental results obtain the spatial structure information and 3D image of the brain stem nuclei, show spatial relationship between 14 pairs of nuclei, and quantitate morphological parameters of each type of nuclei's 3D structure. This work is significant to neuroanatomy research and clinic applications. Furthermore, a software system named BRAIN.HUK is established.

Keywords: Brain stem nuclei, centroid registration, 3D reconstruction, 3D structure quantification

1. Introduction

The thalamus is complicatedly composed of many nuclei and it is difficult to recognize the nuclei's spatial structure [14]. In neuroanatomy, each type of nuclei's morphometrics is generally analyzed and understood by sectioning. Thus, it is quite necessary to study the brain stem nuclei's spatial structure, to obtain 3D image and profile plan of reconstructed nuclei, to show spatial relationship between all sorts of nuclei and to quantification analyze each type of nuclei's morphometrics. The serial sections of the brain stem, i.e. the left and right thalami and its 14 pairs of nuclei, were digitally imaged by CCD camera. By image processing the serial binary images were obtained. After 3D reconstruction, the brain stem nuclei can be shown on arbitrary profile plane in 3D space, and the spatial relationship between the nuclei is revealed. For the moment 3D reconstruction can solve the spatial structure of the nuclei, but in techniques of 3D reconstruction there exist some problems such as auto-registration and precise alignment [2,3,15,18]. This paper introduces an algorithm of fast auto-registration and alignment based on centroidal coordinates of the nuclei. The 3D reconstruction of the brain stem nuclei mainly involves the following steps [4,8,12]:

*Corresponding author: Kuanghu Hu, Institute of Biophysics, Chinese Academy of Sciences, 15 Datun Road, Chaoyang District, Beijing 100101, P.R. China. Tel.: +86 10 64888589; Fax: +86 10 64877837; E-mail: hukh@sun5.ibp.ac.cn.

- To extract contours and centroids of the brain stem nuclei in serial section images.
- Using the characteristic that centroids of the brain stem nuclei in two adjacent section images should be continuous, to adjust translational and rotational offsets between sections; Then, based on mean least distance criterion of multiple objects and three-point pattern registration of centeroids in adjacent sections, the optimal aligning for contours of nuclei was achieved.
- Introducing centroids of nuclei as reference points between serial sections, auto tracing multiple objects in two adjacent sections, to reconstruct the 3D structure of the brain stem nuclei.

The algorithms of object registration, local search, point correspondence alignment, image processing and identification were completed and their corresponding functional modules were established. Thus, by connecting each module we developed a whole software system named BRAIN.HUK which realizes a new approach for 3D reconstruction of the brain stem nuclei from serial sections. The experimental results show that this software system has good performances, and it is significant to neuroanatomy research and clinic applications.

2. Materials and methods

2.1. Preparation of samples

Six mature rats (both sexes) were selected with weight 180–250 g. The brain stem and the thalamus was fixed in mixture solution of 2% paraformaldehyde, 2.5% glutaraldehyde, 0.02–0.1% picric acid and embedded into celloidin. Then the samples were serially sectioned by coronal direction. 155 sections were obtained with 50 μm thickness each, which show 14 pairs of nuclei and the brain stem. i.e., spinal nucleus of trigeminal nerve (sections 1–58), nucleus of hypoglossal nerve (9–38), dorsal nucleus of vagus nerve (13–38), inferior olivary nucleus (13–34), nucleus of facial nerve (35–68), nervus medial vestibular nucleus (39–72), pontine nucleus of trigeminal nerve (55–78), nervus latel vestibular nucleus (57–72), nucleus of abducens nerve (69–72), motorial nucleus of trigeminal nerve (69–84), mesencephalic nucleus of trigeminal nerve (74–143), nervus trochlear nucleus (116–121), nervus oculomotor nucleus (122–155), red nucleus (130–155).

2.2. Methods

After being magnified by WILD M3 SERUES anatomical microscope (objective lens 1.8×), the sections of the brain stem nuclei were digitally imaged by CCD camera. Quantitative analysis and image processing were accomplished on PC Pentium IV-1.7G by using VC++5.0 in Windows 98. The images obtained are 512 × 512 pixels in size with 256 gray levels.

3. Image processing and algorithms

3.1. Extracting contours from images of the brain stem and the nuclei

The images obtained have 256 gray levels, with the grayscale value $g = 0, 1, \ldots, 255$. The probability of g is $P(g) = N(g)/M$, where $N(g)$ is the number of pixels with the grayscale value g, and M is the

total number of pixels in the image. The entropy is defined as

$$ETY = -\sum_{g=0}^{255} P(g) \lg P(g). \tag{1}$$

Based on the distribution of the entropy and two-peak threshold value T the brain stem background and the nuclei were segmented [7,16]. When the image histogram exhibits two peaks T can be computed by a quadratic equation:

$$C_1 T^2 + C_2 T + C_3 = 0, \tag{2}$$

where

$$C_1 = \sigma_1^2 - \sigma_2^2,$$
$$C_2 = 2(\alpha_1 \sigma_2^2 - \alpha_2 \sigma_1^2),$$
$$C_3 = \alpha_2^2 \sigma_1^2 - \alpha_1^2 \sigma_2^2 + \sigma_1^2 \sigma_2^2 \ln\left(\frac{\sigma_2 P_1}{\sigma_1 P_2}\right),$$

where α_1, α_2 are respectively the mean grayscale values of the brain stem background and the nuclei region, σ_1, σ_2 are respectively the root-mean-square deviation of two peaks, and P_1, P_2 are respectively the probabilities of two peaks. After the solution to this quadratic equation is obtained as the optimal threshold value, the binary images of the brain stem background and the nuclei region are defined as

$$f'(x,y) = \begin{cases} 1, & G_1 \leqslant f(x,y) \leqslant T, \\ 0, & T \leqslant f(x,y) \leqslant G_2, \end{cases} \tag{3}$$

where $f(x,y)$ is the function of grayscale images of the brain stem and the nuclei, its values range from G_1 to G_2, the segmentation threshold value T is between G_1 and G_2. Figure 1 is the binary images of 14 types of nuclei selected from 155 sections.

3.2. *Alignment for translation and rotation*

Using the characteristic that centroids of the brain stem nuclei in two adjacent section images should be continuous, the serial section images were aligned to a good extent. Then, based on mean least distance criterion of multiple objects in adjacent sections, the optimal aligning for contours of nuclei was achieved.

Serial section images must be aligned exactly [11,13], while traditional artificial fiducial point alignment has big errors and degrades image quality. In order to correct translational and rotational offsets which came from serial sectioning and imaging, the relative locations of objects in adjacent section images were adjusted. The algorithm of translating and rotating images is formulated as follows:

$$H_\theta = \sum_i \sum_j (i \cos\theta - j \sin\theta)^2 f_\theta(x,y), \tag{4}$$

where θ is rotational angle.

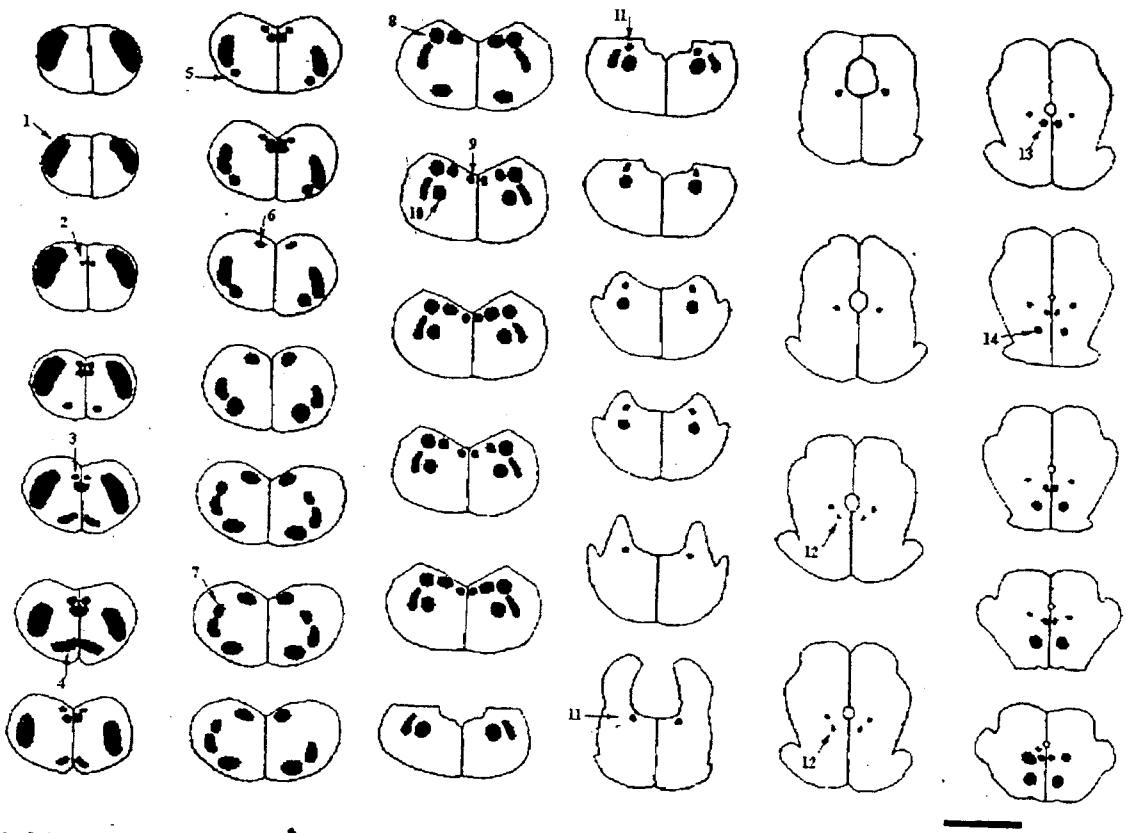

Fig. 1. Selecting representative section images of 14 pairs of nuclei from 155 section images: 1 – spinal nucleus of trigeminal nerve; 2 – nucleus of hypoglossal nerve; 3 – dorsal nucleus of vagus nerve; 4 – inferior olivary nucleus; 5 – nucleus of facial nerve; 6 – nervus medial vestibular nucleus; 7 – pontine nucleus of trigeminal nerve; 8 – nervus latel vestibular nucleus; 9 – nucleus of abducens nerve; 10 – motorial nucleus of trigeminal nerve; 11 – mesencephalic nucleus of trigeminal nerve; 12 – nervus trochlear nucleus; 13 – nervus oculomotor nucleus; 14 – red nucleus. Scale bar = 5 mm.

3.3. *Algorithm of extracting centroid points*

We extracted the centroids of the brain stem nuclei from each section image [19,20]. For a digital $N \times N$ image $f(i,j)$, the coordinate of its centroid (x_c, y_c) can be computed by central moment:

$$\begin{aligned} f(i,j) &= \begin{cases} 1, & (i,j) \in \text{object}, \\ 0, & (i,j) \notin \text{object}, \end{cases} \\ x_c &= m(1,0)/m(0,0), \\ y_c &= m(0,1)/m(0,0), \end{aligned} \tag{5}$$

where

$$m(u,v) = \sum_{i=1}^{N} \sum_{j=1}^{N} f(i,j) i^u j^v.$$

Obviously, x_c and y_c are the mean of abscissa and ordinate of the points in the object respectively. The following can be obtained from probability statistics:

$$\begin{aligned} D_x &= \sum_{i=1}^{N}(x_i - x)^2 \quad \text{when } x = x_c,\ D_x \text{ reaches the minimum,} \\ D_y &= \sum_{i=1}^{N}(y_i - y)^2 \quad \text{when } y = y_c,\ D_y \text{ reaches the minimum,} \end{aligned} \tag{6}$$

where x_i and y_i satisfy $f(x_i, y_i) = 1$. Combining D_x and D_y we obtains:

$$D_x + D_y = \sum_{i=1}^{N}(x_i - x_c)^2 + \sum_{i=1}^{N}(y_i - y_c)^2 = \sum_{i=1}^{N}[(x_i - x_c)^2 + (y_i - y_c)^2], \tag{7}$$

where $[(x_i - x_c)^2 + (y_i - y_c)^2]$ is actually the square of the distance between the point (x_i, y_i) in the object and the centroid (x_c, y_c). Obviously, $D_x + D_y$ reaches the minimum at (x_c, y_c), that is to say, the sum of the distances between the centroid and each point in the object is the smallest [5].

3.4. 3D image registration

There are two methods for image registration. One is based on grayscale information of individual pixel or pixels in certain regions, and the other is based on feature space information (contour information, transformation space information) [1,17].

3D reconstruction must accomplish registration and alignment of centroids and contours of the nuclei and auto-tracing of identical object [6,9]. 14 pairs of the brain stem nuclei were serially sectioned by coronal direction. Thus 155 sections were obtained, which show 14 pairs of nuclei and the brain stem. The locations of the centroids of nuclei in adjacent section images should be continuous. In fact there are at least 3 correspondence centroid points in each section image. This provides three-point pattern registration. The corresponding centroidal coordinates of the nuclei (x_{j1}, y_{j1}), (x_{j2}, y_{j2}), (x_{j3}, y_{j3}) and (x_{k1}, y_{k1}), (x_{k2}, y_{k2}), (x_{k3}, y_{k3}) between two adjacent sections f_j $(j = 1, 2, \ldots, n)$ and f_k $(k = j + 1)$ are well matched on the whole. 14 pairs of nuclei are distributed on different spatial locations and thus the three-point pattern registration requires auto selecting different nuclei in each section. Quite few sections have only one pair of nuclei. In this case, the centroid of the brain stem contour should be used as one of the three reference points. As a matter of fact, in most section images there are several pairs of nuclei's centroids which can be regarded as corresponding points.

3.4.1. Centroid three-point pattern registration

Between serial sections the centroids of the brain stem nuclei were introduced as reference points. Two adjacent section images were considered as the original image and the fiducial image in which the centroidal coordinates are separately (x_i, y_i) and (φ_i, γ_i), $i = 1, 2, \ldots, N$. Registration was performed by using least square error criterion. Geometric transformation between these two images was represented by the bivariate quadratic polynomials:

$$\begin{aligned} \varphi &= q_{00} + q_{10}x + q_{01}y + q_{11}xy + q_{20}x^2 + q_{02}y^2, \\ \gamma &= h_{00} + h_{10}x + h_{01}y + h_{11}xy + h_{20}x^2 + h_{02}y^2. \end{aligned} \tag{8}$$

The registration for the original image and the fiducial image can be converted into the computation of the least square solution Q and H from an equation set as follows:

$$\begin{aligned} \Omega Q &= G, \\ \Omega H &= K, \end{aligned} \tag{9}$$

where

$$\begin{aligned} Q &= [q_{00}\ q_{10}\ q_{01}\ q_{11}\ q_{20}\ q_{02}]^T, \\ H &= [h_{00}\ h_{10}\ h_{01}\ h_{11}\ h_{20}\ h_{02}]^T, \\ G &= [\varphi_1\ \varphi_2 \ldots \varphi_N]^T, \\ K &= [\gamma_1\ \gamma_2 \ldots \gamma_N]^T, \\ \Omega &= \begin{vmatrix} 1 & x_1 & y_1 & x_1y_1 & x_1^2 & y_1^2 \\ 1 & x_2 & y_2 & x_2y_2 & x_2^2 & y_2^2 \\ \vdots & \vdots & \vdots & \vdots & \vdots & \vdots \\ 1 & x_N & y_N & x_Ny_N & x_N^2 & y_N^2 \end{vmatrix}. \end{aligned} \tag{10}$$

The solutions are:

$$\begin{aligned} Q &= (\Omega^T\Omega)^{-1}\Omega^T G, \\ H &= (\Omega^T\Omega)^{-1}\Omega^T K. \end{aligned} \tag{11}$$

Tests indicated that the algorithm obtains a good result on alignment and registration of contours and centroids of the brain stem nuclei.

3.4.2. Matching of nuclei's contours between adjacent sections

Assuming $f_j(x, y)$ and $f_k(x, y)$ are both continuous intensity functions, the $F(i, j)$ and $S(i, j)$ separately represent the transformed image and the reference image with size of $N \times N$. The objective function Δ is the quadratic sum of residual error of $F(i, j)$ and $S(i, j)$:

$$\Delta = \sum_i \sum_j (F(i, j) - S(i, j))^2. \tag{12}$$

The objective function Δ represents the similarity of two images, and the departure of centroidal coordinates of the nuclei in adjacent section images [10].

4. Results and discussion

4.1. 3D structure and spatial configuration of the brain stem nuclei

This paper established a 3D reconstruction method of the brain stem nuclei based on fast centroid auto-registration, and quantitative analysis was accomplished with computer image processing. With entropy distribution and two-peak threshold value T, the fine contours of the nuclei structure and the brain stem were extracted. The algorithms and functional modules thereof for object registration, local search, point

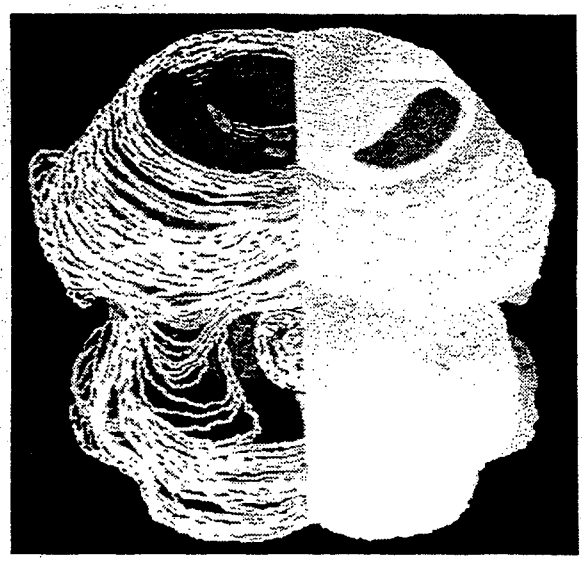

Fig. 2. The 3D shape generated from the contours of the brain stem.

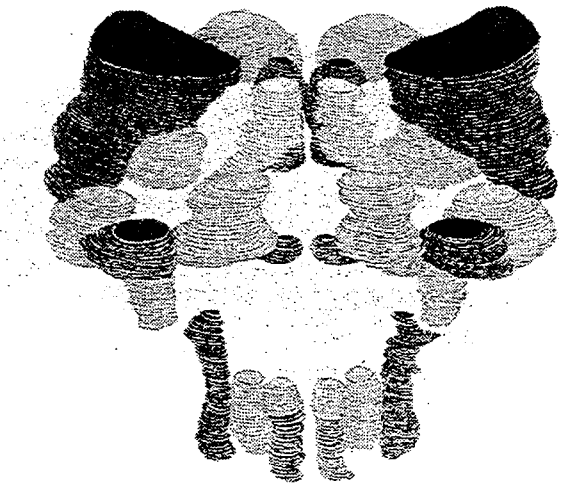

Fig. 3. The spatial structure of 14 pairs of nuclei is shown by 3D reconstruction.

correspondence alignment, image processing and identification were completed. Then these modules were connected into a whole software system, which realize a new method for 3D reconstruction of the brain stem nuclei from serial sections. Figures 2 and 3 are separately the shape of the brain stem and the spatial structure of 14 pairs of nuclei.

4.2. *Quantitative parameters of 3D structure of the brain stem and the nuclei*

The volume of the brain stem nuclei is represented by the expression:

$$V = \frac{A \cdot t \cdot d}{Rx \cdot Ry}, \tag{13}$$

Table 1
Feature parameters of the brain stem nuclei

Serial number	Nuclei type	Section number of nuclei	Nuclei pair volume (mm^3)	Volume ratio of nuclei to brain stem (%)	Nuclei extent (mm)
1	Spinal nucleus of trigeminal nerve	58	9.92	7.11	2.9
2	Nucleus of hypoglossal nerve	30	1.32	0.95	1.5
3	Dorsal nucleus of vagus nerve	26	0.33	0.24	1.3
4	Inferior olivary nucleus	22	2.04	1.46	1.1
5	Nucleus of facial nerve	34	5.03	3.61	1.7
6	Nervus medial vestibular nucleus	18	3.59	2.57	0.9
7	Pontine nucleus of trigeminal nerve	34	6.36	4.56	1.7
8	Nervus latel vestibular nucleus	16	1.45	1.04	0.8
9	Nucleus of abducens nerve	4	0.07	0.05	0.2
10	Motorial nucleus of trigeminal nerve	16	0.89	0.64	0.8
11	Mesencephalic nucleus of trigeminal nerve	70	1.26	0.90	3.5
12	Nervus trochlear nucleus	6	0.09	0.06	0.3
13	Nervus oculomotor nucleus	34	0.49	0.35	1.7
14	Red nucleus	26	1.12	0.80	1.3

where A is the sum of all sectional areas of one pair of nuclei, t is the section thickness, d is the section interval (to serial sections, $d = 1$), R_x, R_y are separately magnification factor of X and Y axis.

As shown in Table 1, the volumes of the brain stem nuclei, the nuclei extent and the percentage of the nuclei volume to the brain stem volume were obtained for six rats. The volume of the brain stem measured is 139.49 ± 4.51 mm^3. The maximum volume of nuclei pair (spinal nucleus of trigeminal nerve) is 9.92 mm^3 and its percentage to the brain stem is 7.71%. Nucleus of abducens nerve has the minimum volume as 0.07 mm^3, and its percentage to the brain stem is 0.05%. The volume ratio of the maximum nuclei pair to the minimum is about 142.

5. Conclusion

By automatically selecting three nuclei's centroids as feature points for auto-registration in serial section images, we established a 3D reconstruction of the brain stem nuclei based on fast centroid auto-registration. Based on methods and theories of computer stereo vision this research accomplishes local search, registration and auto-tracing for the centroids of the brain stem nuclei and establishes a new 3D reconstruction technique. Reconstructed results show spatial relationship between 14 pairs of nuclei and obtain quantitative morphological parameters of each pair of nuclei. This work provides an important technique for further research on the relationship between structure and function of the brain stem nuclei. Meanwhile, a software system named BRAIN.HUK is established. Our methods and software system are significant to neuroanatomy research and clinic applications.

Acknowledgement

This project is funded by National Natural Science Foundation of China (No. 39320217, 39970217).

References

[1] B.J. Ross and E.M. Riseman, How easy is matching 2D line models using local search, *IEEE PAMI* **19**(6) (1997), 564–579.
[2] D. Gavrila and L. Davis, 3-D model-based tracking of humans in action: a multi-view approach, in: *Proc. of IEEE Conference on Computer Vision and Pattern Recognition*, San Francisco, 1996, pp. 73–80.
[3] D. Terzopoulos and D. Metaxas, Dynamic 3-D models with local and global deformations: deformable superquadrics, *IEEE Trans. Pattern Analysis and Machine Intelligence* **13** (1991), 703–714.
[4] F. Caliò, G. Moroni and M. Rasella, A particular class of spline in reconstruction of revolution surfaces from 3-D data measured by CMM, *Robotics and Computer-Integrated Manufacturing* **19**(1) (2003), 219–224.
[5] F.Z. Li, K.H. Hu and W.F. Su, Automatic recognition of small cell carcinoma based on the self-organizing neural network, *Bio-Medical Materials and Engineering* **14**(2) (2004), 175–184.
[6] H. Li, B.S. Manjunath and S.K. Mitra, A contour-based approach to demultisensor image registration, *IEEE Trans. on Image Processing* 4(3) (1995), 320–334.
[7] H.T. Xiong, K.H. Hu, W.F. Su et al., Automatic quantitative analysis of bipolysaccharide liposome by image processing method, *Bio-Medical Materials and Engineering* **14**(2) (2004), 175–184.
[8] J. Celles, J. Bruce and M.P. Sheetz, Tracking kinesin-driven movements with nanometer-scale precision, *Nature* **331** (1998), 450–453.
[9] J.K. Aggarawal, Q. Cai, W. Liao et al., Non-rigid motion analysis: articulated and elastic motion [J], *Computer Vision and Image Understanding* **70**(2) (1998), 142–156.
[10] J.T. Vincent, Van Ginneken, D.F. Albert, Addink et al., Metabolic rate and level of activity determined in tilapia by direct and indirect calorimetry and video monitoring [J], *Thermochimica Acta* **291** (1997), 1–13.
[11] J.V. Hanjnal, N. Saeed, E.J. Soar et al., A registration and interpolation procedure for subvoxel matching of serially acquired MR image, *J. Comput. Assist. Tomog.* **19** (1995), 289–296.
[12] J.W. Dai and M.P. Sheetz, Cell membrane mechanics, *Methods in Cell Biology* **55** (1998), 157–160.
[13] K.J. Friston, J. Ashburner, C.D. Frith et al., Spatial registration and normalization of images, *Human Brain Mapping* 3 (1995), 165–189.
[14] M.B. Carpenter, *Human Neuroanatomy*, Williams & Wilkins, Baltimore, 1976, p. 442.
[15] M. Seibert and A.M. Waxman, Adaptive 3D object recognition from multiple views, *IEEE Trans Pattern Analysis and Machine Intelligence* **14**(7) (1992), 107–124.
[16] N. Cai, K.H. Hu, H.T. Xiong et al., Image segmentation of G bands of Triticum monococcum chromosomes based on MBNN, *Pattern Recognition Letters* **25**(3) (2004), 319–329.
[17] R. Douglas, Heisterkamp, prabir bhattacharya, Matching 2D polygonal arcs by using a subgroup of the unit quaternions, *Computer Vision and Image Understanding* **69**(2) (1998), 246–249.
[18] R. Okada, Y. Shirai and J. Miura, Tracking a person with 3-D motion by integrating optical flow and depth, in: *The Fourth International Conference on Automatic Face and Gesture Recognition*, Grenoble, France, 2000.
[19] S.Y. Li, K.H. Hu, W.F. Su et al., Automatic analysis of image of surface structure of cell wall-deficit EVC, *Bio-Medical Materials and Engineering* **11**(3) (2001), 159–166.
[20] S.Y. Li, K.H. Hu, W.F. Su et al., Automatic quantitative analysis of ore content of human tooth enamel by mask image scanning method, *Bio-Medical Materials and Engineering* **13**(4) (2003), 363–371.